Induced Ti magnetization at La0.7Sr0.3MnO3 and BaTiO3 interfaces

Yaohua Liu, J. Tornos, S. G. E. te Velthuis, J. W. Freeland, H. Zhou, P. Steadman, P. Bencok, C. Leon, and J. Santamaria

Articles you may be interested in

The effect of interface roughness on exchange bias in La0.7Sr0.3MnO3–BiFeO3 heterostructures
Appl. Phys. Lett. **108**, 072401 (2016); 10.1063/1.4941795

Magnetic properties of BaTiO3/La0.7Sr0.3MnO3 thin films integrated on Si(100)
J. Appl. Phys. **116**, 224104 (2014); 10.1063/1.4903322

Charge control of antiferromagnetism at PbZr0.52Ti0.48O3/La0.67Sr0.33MnO3 interface
Appl. Phys. Lett. **104**, 132905 (2014); 10.1063/1.4870507

Electric modulation of magnetization at the BaTiO3/La0.67Sr0.33MnO3 interfaces
Appl. Phys. Lett. **100**, 232904 (2012); 10.1063/1.4726427

Coexistence of tunneling magnetoresistance and electroresistance at room temperature in La0.7Sr0.3MnO3/(Ba, Sr)TiO3/La0.7Sr0.3MnO3 multiferroic tunnel junctions
J. Appl. Phys. **109**, 07D915 (2011); 10.1063/1.3564970

Induced Ti magnetization at La$_{0.7}$Sr$_{0.3}$MnO$_3$ and BaTiO$_3$ interfaces

Yaohua Liu,[1,2,a] J. Tornos,[3] S. G. E. te Velthuis,[2] J. W. Freeland,[4] H. Zhou,[4] P. Steadman,[5] P. Bencok,[5] C. Leon,[3] and J. Santamaria[3]

[1]*Quantum Condensed Matter Division, Oak Ridge National Laboratory, Oak Ridge, Tennessee 37831, USA*
[2]*Materials Science Division, Argonne National Laboratory, Argonne, Illinois 60439, USA*
[3]*GFMC, Instituto de Magnetismo Aplicado, Universidad Complutense Madrid, 28040 Madrid, Spain*
[4]*Advanced Photon Source, Argonne National Laboratory, Argonne, Illinois 60439, USA*
[5]*Diamond Light Source, Science Division, Didcot OX11 0DE, United Kingdom*

In artificial multiferroics hybrids consisting of ferromagnetic La$_{0.7}$Sr$_{0.3}$MnO$_3$ (LSMO) and ferroelectric BaTiO$_3$ epitaxial layers, net Ti moments are found from polarized resonant soft x-ray reflectivity and absorption. The Ti dichroic reflectivity follows the Mn signal during the magnetization reversal, indicating exchange coupling between the Ti and Mn ions. However, the Ti dichroic reflectivity shows stronger temperature dependence than the Mn dichroic signal. Besides a reduced ferromagnetic exchange coupling in the interfacial LSMO layer, this may also be attributed to a weak Ti-Mn exchange coupling that is insufficient to overcome the thermal energy at elevated temperatures. © *2016 Author(s). All article content, except where otherwise noted, is licensed under a Creative Commons Attribution (CC BY) license (http://creativecommons.org/licenses/by/4.0/).* [http://dx.doi.org/10.1063/1.4946756]

Complex oxide interfaces can host fundamentally new physics and novel functionalities.[1–4] For example, metallicity, superconductivity, and ferromagnetism have all been found serendipitously at interfaces between insulating and non-magnetic oxides.[5–7] At interfaces between a ferromagnetic manganite and a superconducting or non-superconducting cuprate, interface-induced Cu spin polarization significantly changes the spin dependent transport properties.[8,9] Similarly at interfaces between ferromagnetic and ferroelectric oxides novel forms of magnetoelectric coupling may occur.[10] It has been shown that when a magnetic oxide layer is interfaced with a ferroelectric layer, its interfacial magnetism can be modulated by the ferroelectric polarization.[11,12] Since spin dependent transport is very sensitive to interfacial magnetism, magnetic tunnel junctions with a ferroelectric oxide barrier can be engineered to control the spin dependent tunnel conductance by electric fields.[13–15] The interfacial magnetism can be altered due to strain, charge transfer, orbital reconstruction, octahedral rotation, ionic diffusion, or a combination of these.[16–21] Thus, knowledge on the interfacial properties and its tunability is crucial for utilizing ferromagnet/ferroelectric heterostructures for spintronics.

Here we report the unexpected Ti magnetization in heterostructures consisting of ferromagnetic La$_{0.7}$Sr$_{0.3}$MnO$_3$ (LSMO) and ferroelectric BaTiO$_3$ (BTO) via circularly polarized resonant soft x-ray reflectivity and absorption experiments. Magnetic dichroic signals at both the Ti and Mn *L* edges follow each other during the magnetization reversal, which indicates an induced Ti magnetization that is of interfacial origin and exchange-coupled to the Mn magnetization. We have also found that the Ti dichroic reflectivity decays faster than the Mn signal on heating, which can be explained by either a weak Ti-Mn exchange coupling or a reduced ferromagnetic exchange coupling in the interfacial LSMO layer adjacent to BTO.

[a]liuyh@ornl.gov

4, 046105-1

The four bilayer samples consist of nominally 10 nm $La_{0.7}Sr_{0.3}MnO_3$ (LSMO) grown on $SrTiO_3$ (STO) substrates, capped by t nm $BaTiO_3$ (BTO) with $t = 1.2, 1.2, 2.4$, and 4.8 nm, respectively. Bulk LSMO is ferromagnetic and bulk BTO is ferroelectric at room temperature. We have also studied a 13 nm BTO single layer sample and a trilayer sample with the nominal structure of 7 nm LSMO/ 4.4 nm BTO/ 25 nm LSMO // STO. These samples were fabricated via high pressure pure O_2 sputtering deposition. This technique has proven to yield good epitaxial growth of complex oxides.[22,23] X-ray reflectometry studies show that the LSMO-BTO interface roughnesses are 1–2 u.c. in these bilayers. Negligible Mn-Ti intermixing was found within instrument resolution with atomic column resolution STEM EELS. Piezoresponse force microscopy studies show that the ferroelectric polarization of these bilayers is preferably pointing down. However, as-prepared samples were used for the x-ray studies reported below and the ferroelectric polarization of the BTO layer was in a multi-domain state. High resolution x-ray diffraction experiments and circularly polarized soft x-ray resonant reflectivity experiments were performed at beamlines 11-ID-D and 4-ID-C, respectively, at the Advanced Photon Source (APS). X-ray resonant absorption experiments for measuring magnetic circular dichroism were performed at BL I10 at the Diamond Light Source (DLS). Polarized x-ray data presented below are from one of the 1.2 nm BTO samples, except as explicitly noted.

High resolution x-ray diffraction experiments are performed to characterize the structure of the films. Figure 1(a) shows an out-of-plane L scan across the substrate (1 0 2) off-specular peak from the 4.8 nm BTO bilayer. The average c-axis lattice constants are 0.385 nm for LSMO and 0.415 nm for BTO, respectively. Figures 1(b)-1(d) show the in-plane H scans near the (1 0 2) Bragg peaks from BTO, STO substrate, and LSMO, respectively. From the peak positions in the H scans, we find that the average in-plane lattice mismatches are $0.17\% \pm 0.02\%$ between BTO and STO, and $-0.01\% \pm 0.01\%$ between LSMO and STO. Therefore the LSMO layer is almost fully strained and the BTO layer is slightly relaxed. The relaxation of the BTO layer is likely due to the large lattice mismatch between BTO and STO. Overall, the LSMO layer is under in-plane tensile strain and the BTO layer is under in-plane compressive strain.

We have utilized dichroic interference effects in circularly polarized resonant x-ray reflectivity[24,25] to study the element-specific magnetization. At APS beamline 4-ID-C, the instrumental configuration allows measurement of x-ray reflectivity as a function of energy via switching the photon helicity at each energy.[26] During the experiments, a magnetic field was applied either parallel or antiparallel to the propagation direction of the incident x-rays. The sum of the reflected intensities $(I^+ + I^-)$ of these signals provides information on the electronic environment of the probed element, while magnetic information is contained in the dichroic signal $(I^+ - I^-)$.[25]

Figures 2(a) and 2(b) show the dichroic reflectivity at the Mn and Ti L edges from the 1.2 nm BTO bilayer. The reflectivity data were collected at 60 K in magnetic fields of ± 2 kOe with an x-ray incident angle of 10°. As expected, there is a large Mn dichroic signal. Interestingly, there is
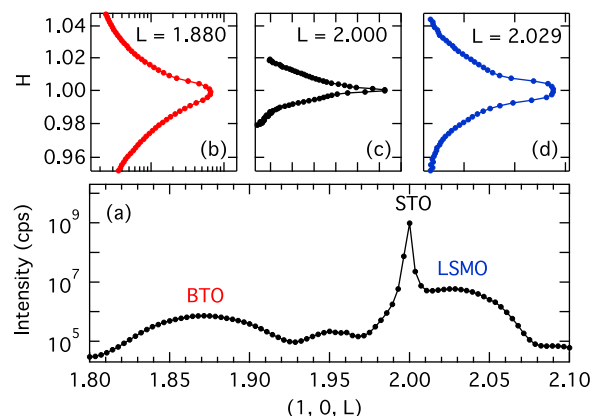

FIG. 1. High resolution x-ray diffraction data taken from the 4.8 nm BTO bilayer. (a) Out-of-plane L scan across the (1 0 2) peak of the STO substrate. (b)-(d) In-plane H scans around the Bragg peaks from BTO, STO substrate, and LSMO.
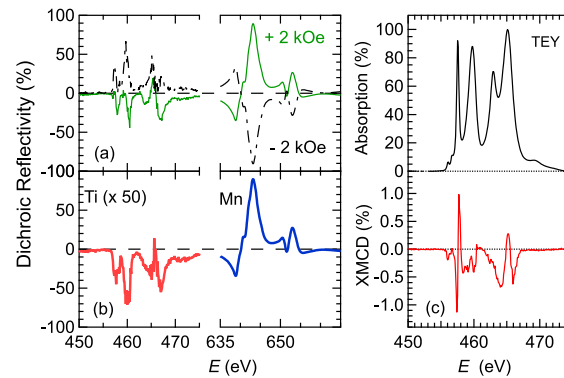
FIG. 2. Dichroic reflectivity as a function of photon energy at the Ti and Mn L edges on the 1.2 nm BTO sample. (a) The dichroic reflectivity measured with circularly polarized x-rays in +2 kOe (solid) and −2 kOe (dashed) fields, respectively. (b) Difference of the dichroic reflectivities taken in ±2 kOe fields. (c) X-ray absorption and magnetic circular dichroism at Ti L edge taken from the second 1.2 nm bilayer. Data were collected with ±5 T out-of-plane field at 10 K.

also a notable Ti dichroic signal. In bulk stoichiometric BTO, Ti^{4+} ions have no d electrons and no significant magnetic signal is expected. After switching the field from +2 kOe to −2 kOe, the Mn dichroic signal was almost fully reversed and the Ti dichroic signal was largely reversed. To remove the possible experimental artifacts and thus better reflect the magnetic contribution, the difference between the two dichroic curves taken at positive and negative fields will be used as the dichroic reflectivity reported below. Significant Ti dichroic reflectivity signals have been observed in all bilayer and trilayer samples, but not for the single BTO layer sample. This excludes the native oxygen vacancies as the major origin of the observed net Ti moment, in contrast to the $LaAlO_3/SrTiO_3$ interface.[27] However, accumulation of oxygen vacancies at the interface (for example to relieve the large epitaxial mismatch strain) may be a source of electron doping responsible for the Ti magnetism. Therefore, the observed Ti dichroic signal is not intrinsic to the BTO film but is due to the existence of the adjacent LSMO layer. In the literature, induced Ti magnetization in $BaTiO_3$ has been reported when it interfaces with transition-metal ferromagnets,[28] and it has been found that the interfacial Ti-O-Mn covalent bonding can give rise to magnetic Ti ions at layered manganite-titanate interfaces.[2,27,29]

Below, we will provide more evidence of magnetic Ti ions at LSMO/BTO interfaces. Note that the bilayer was grown on top of a STO substrate, which contains a LSMO/STO interface (as well as a LSMO/BTO interface) that may contain magnetic Ti ions[29] and contribute to the dichroic reflectivity signal. To lift the uncertainty, we measured x-ray magnetic dichroism (XMCD) via the total electron yield (TEY) mode at beamline I10, DLS. Figure 2(c) shows the x-ray absorption and XMCD data at Ti L edge from a second 1.2 nm BTO bilayer. A 50 kOe out-of-plane magnetic field was applied during collecting the absorption spectra with the two different x-ray helicities. Then the field was changed to −50 kOe field and the measurements were repeated. All these data were used to obtain the average signal. The data show clear dichroic TEY signals at the Ti L edge. The TEY mode is near-surface sensitive with a limited probing depth about 2-5 nm. Note that the LSMO layer is 10 nm thick; thus, the Ti TEY signal is essentially from the top BTO layer. Therefore, the result proves that there are indeed magnetic Ti ions at the LSMO/BTO interface. A rough estimate of the magnitudes via applying sum rules[30] shows that the spin and orbital moments are −0.04 μ_B and 0.03 μ_B per Ti ion, assuming a uniform distribution of the Ti moment in the BTO layer. The observed finite net Ti moment reveals non-zero Ti $3d$-orbital occupation.[27] The negative Ti spin moment indicates that it is antiparallel to the Mn magnetization, the same as that observed at the LSMO/STO interface.[29]

To explore the origin of the magnetic Ti ions, we have measured element-specific hysteresis loops. Figure 3(a) shows the data from the 1.2 nm bilayer in an in-plane magnetic field, which were taken at 30 K at 466.0 eV and 641.7 eV to probe the Ti and Mn magnetization, respectively. The Ti signal follows the Mn signal during the magnetization reversal, which indicates that the Ti and Mn ions are exchange coupled. Figure 3(b) shows the data from the trilayer. The Mn hysteresis
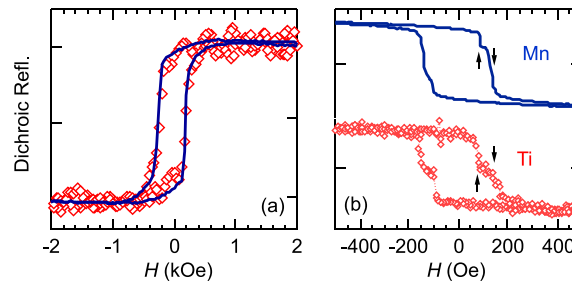
FIG. 3. Magnetic hysteresis loops measured with the dichroic reflectivity. (a) Data taken from the 1.2 nm bilayer at Ti *L* edge (466.0 eV, open diamond) and Mn *L* edge (641.7 eV, solid line), respectively. The Ti signal closely follows the Mn signal. (b) Data taken from the trilayer sample at Ti *L* edge (465.0 eV, open diamond) and Mn *L* edge (642.0 eV, solid line), respectively. Both Mn and Ti signals show two-step switching behavior during the magnetization reversal.

loop shows two switchings, corresponding to the magnetization reversals of the top and bottom LSMO layers, respectively. This is because the top and bottom manganite layers have different coercivities, likely due to different strain states. The Ti loop shows two switchings at the same fields as observed in the Mn loop. This indicates that LSMO grown on the top of BTO can also induce a Ti magnetization. Overall, these observations lead to the conclusion that the observed Ti magnetization is of interfacial origin.

Figure 4(a) shows dichroic reflectivity of the 1.2 nm bilayer sample taken with ±2 kOe fields at 60 K (solid lines) and 270 K (dashed lines), respectively. There are clear changes in the lineshape of the Mn dichroic reflectivity between 60 K and 270 K. In contrast, the Mn dichroic TEY signal barely changes the lineshape with temperature, as shown in Fig. 4(b). This is because the dichroic TEY probes the near-interface Mn magnetization, and the dichroic reflectivity is sensitive to the depth profiles of Mn magnetization.[25] If there was a magnetization redistribution as a function of depth but the average Mn magnetization remained unchanged, the dichroic reflectivity would show more changes in the line-shape rather than amplitude, but the dichroic TEY would show more changes in its amplitude rather than its lineshape.
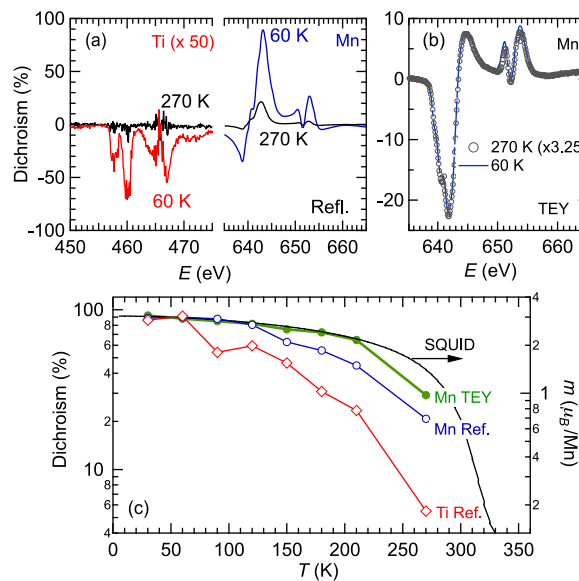

FIG. 4. (a) Dichroic reflectivity at both the Ti and Mn *L* edges. Date were taken from the 1.2 nm bilayer in ±2 kOe fields at 60 K (solid lines) and 270 K (dashed lines), respectively. (b) Dichroic TEY signal at the Mn *L* edge. (c) Temperature dependence of the dichroic TEY at the Mn *L* edge (solid circles, multiplied by a factor of 4), and the dichroic reflectivity taken at the Mn (circle) and Ti (diamond, multiplied by a factor of −200) *L* edges, respectively. Also plotted is the average magnetization data collected in a 1 kOe in-plane field.

Figure 4(c) summarizes the temperature dependence of the element-specific dichroic signals. For Ti, the integrated dichroic reflectivity in the range between 455 and 475 eV is given to improve the signal to noise ratio. For Mn, the peak values near 643 eV are used. The average magnetization measured in a 1 kOe in-plane field with a superconducting quantum interference device (SQUID) magnetometer is also plotted, which shows that T_c of the film is around 320 K. The Mn dichroic signals, both in TEY and reflectivity, show a stronger temperature dependence than the average magnetization determined from SQUID, suggesting a reduced Mn magnetization at the interface. Note that reduced ferromagnetic exchange interaction at surfaces and interfaces of manganite can give rise to strongly suppressed interfacial magnetization at elevated temperatures.[25,31,32] Particularly, previous spin-resolved photoemission spectroscopy studies show that in LSMO the magnetization in the first 5 Å surface layer decays much faster than the bulk magnetization measured by SQUID and also faster than the near surface magnetization (2-5 nm) measured by x-ray absorption spectroscopy.[31] Thus, the reduced ferromagnetic exchange interaction in the interfacial LSMO, giving rise to changes in the depth profiles of the Mn magnetization as temperature changes, may account for the line-shape changes in the Mn dichroic reflectivity.[33]

As shown in Fig. 4(c), the Ti dichroic reflectivity indicates that the ordering temperature of Ti moments is not far from 270 K, much lower than the T_C of the manganite layer. It is clearer from Fig. 4(a): At 270 K, the Mn dichroic signal is still sizable, but the Ti dichroic signal is at the noise level. Since the Ti magnetization is induced by the exchange coupling to interfacial Mn ions, the Ti dichroic signal reflects the ferromagnetism of the first interfacial LSMO layer as well as the exchange coupling between the interfacial Ti and Mn ions. Therefore, the stronger temperature dependence of Ti magnetization can be caused by a weak Ti-Mn exchange coupling, which becomes insufficient to overcome the thermal energy at elevated temperatures. Alternatively, it can be caused by the effective spin ordering temperature of the interfacial manganite being much lower than its bulk counterpart. The interfacial properties, especially that of the first atomic layer, are usually most crucial for understanding the emergent phenomena and spintronic functionalities in magnetic heterostructures. High resolution real-space measurements on buried interfaces normally involve sample cleavage,[34] in which surface reconstruction is a common concern. Alternatively, as shown above, the dichroic reflectivity from the induced interfacial magnetization can be used as a nondestructive and sensitive probe to investigate the magnetization in the first interfacial LSMO layer. This sensitivity is essentially coming from a combination of the strong multiple scattering in the soft x-ray regime and the grazing incidence geometry.[25]

In summary, we have observed induced Ti magnetization in BTO at interfaces with LSMO via circularly polarized resonant soft-x-ray reflectivity and absorption. The magnetic Ti ions are exchange coupled to the Mn ions in the adjacent LSMO layer. The emergent net Ti moments and exchange coupling between the interfacial Ti and Mn ions may have significance to interpret the spin-dependent transport properties when LSMO and BTO are used as building blocks of spintronic devices. As temperature increases, the Ti dichroic reflectivity decays faster than Mn dichroic reflectivity, and both of them show a stronger temperature dependence than the average magnetization of the bilayers. These results can be attributed to reduced ferromagnetic exchange interaction in the interfacial LSMO. At the same time, a weak Ti-Mn exchange coupling at interface can also give rise to the stronger temperature dependence of Ti dichroic signal.

[1] P. Zubko, S. Gariglio, M. Gabay, P. Ghosez, and J.-M. Triscone, Annu. Rev. Condens. Matter Phys. **2**, 141 (2011).
[2] J. Santamaria, J. Garcia-Barriocanal, Z. Sefrioui, and C. Leon, Int. J. Mod. Phys. B **27**, 1330013 (2013).
[3] J. Chakhalian, J. W. Freeland, A. J. Millis, C. Panagopoulos, and J. M. Rondinelli, Rev. Mod. Phys. **86**, 1189 (2014).

[4] Y. Liu and X. Ke, J. Phys.: Condens. Matter **27**, 373003 (2015).

[5] A. Ohtomo and H. Hwang, Nature **427**, 423 (2004).

[6] N. Reyren, S. Thiel, A. D. Caviglia, L. F. Kourkoutis, G. Hammerl, C. Richter, C. W. Schneider, T. Kopp, A.-S. Ruetschi, D. Jaccard, M. Gabay, D. A. Muller, J.-M. Triscone, and J. Mannhart, Science **317**, 1196 (2007).

[7] A. Brinkman, M. Huijben, M. Van Zalk, J. Huijben, U. Zeitler, J. C. Maan, W. G. Van der Wiel, G. Rijnders, D. H. A. Blank, and H. Hilgenkamp, Nat. Mater. **6**, 493 (2007).

[8] Y. Liu, F. A. Cuellar, Z. Sefrioui, J. W. Freeland, M. R. Fitzsimmons, C. Leon, J. Santamaria, and S. G. E. te Velthuis, Phys. Rev. Lett. **111**, 247203 (2013).

[9] Y. Liu, C. Visani, N. M. Nemes, M. R. Fitzsimmons, L. Y. Zhu, J. Tornos, M. Garcia-Hernandez, M. Zhernenkov, A. Hoffmann, C. Leon *et al.*, Phys. Rev. Lett. **108**, 207205 (2012).

[10] S. Fusil, V. Garcia, A. Barthélémy, and M. Bibes, Annu. Rev. Mater. Res. **44**, 91 (2014).

[11] C. Vaz, J. Hoffman, Y. Segal, J. Reiner, R. Grober, Z. Zhang, C. Ahn, and F. Walker, Phys. Rev. Lett. **104**, 127202 (2010).

[12] H. Lu, T. A. George, Y. Wang, I. Ketsman, J. Burton, C.-W. Bark, S. Ryu, D. Kim, J. Wang, C. Binek *et al.*, Appl. Phys. Lett. **100**, 232904 (2012).

[13] M. Gajek, M. Bibes, S. Fusil, K. Bouzehouane, J. Fontcuberta, A. Barthelemy, and A. Fert, Nat. Mater. **6**, 296 (2007).

[14] E. Tsymbal, A. Gruverman, V. Garcia, M. Bibes, and A. Barthélémy, MRS Bull. **37**, 138 (2012).

[15] Y. Yin, J. Burton, Y. M. Kim, A. Y. Borisevich, S. J. Pennycook, S. Yang, T. Noh, A. Gruverman, X. Li, E. Tsymbal *et al.*, Nat. Mater. **12**, 397 (2013).

[16] J. Chakhalian, J. Freeland, H.-U. Habermeier, G. Cristiani, G. Khaliullin, M. Van Veenendaal, and B. Keimer, Science **318**, 1114 (2007).

[17] P. Yu, J.-S. Lee, S. Okamoto, M. Rossell, M. Huijben, C.-H. Yang, Q. He, J. Zhang, S. Yang, M. Lee *et al.*, Phys. Rev. Lett. **105**, 027201 (2010).

[18] J. Seo, W. Prellier, P. Padhan, P. Boullay, J.-Y. Kim, H. Lee, C. Batista, I. Martin, E. E. Chia, T. Wu *et al.*, Phys. Rev. Lett. **105**, 167206 (2010).

[19] X. Zhai, L. Cheng, Y. Liu, C. M. Schlepütz, S. Dong, H. Li, X. Zhang, S. Chu, L. Zheng, J. Zhang *et al.*, Nat. Commun. **5**, 4283 (2014).

[20] A. Bhattacharya and S. J. May, Annu. Rev. Mater. Res. **44**, 65 (2014).

[21] C. Bi, Y. Liu, T. Newhouse-Illige, M. Xu, M. Rosales, J. Freeland, O. Mryasov, S. Zhang, S. te Velthuis, and W. Wang, Phys. Rev. Lett. **113**, 267202 (2014).

[22] Z. Sefrioui, D. Arias, V. Pena, J. Villegas, M. Varela, P. Prieto, C. León, J. Martinez, and J. Santamaria, Phys. Rev. B **67**, 214511 (2003).

[23] V. Pena, Z. Sefrioui, D. Arias, C. Leon, J. Santamaria, M. Varela, S. Pennycook, and J. Martinez, Phys. Rev. B **69**, 224502 (2004).

[24] C.-C. Kao, C. Chen, E. Johnson, J. Hastings, H. Lin, G. Ho, G. Meigs, J.-M. Brot, S. Hulbert, Y. Idzerda *et al.*, Phys. Rev. B **50**, 9599 (1994).

[25] J. Freeland, J. Kavich, K. Gray, L. Ozyuzer, H. Zheng, J. Mitchell, M. Warusawithana, P. Ryan, X. Zhai, R. Kodama *et al.*, J. Phys.: Condens. Matter **19**, 315210 (2007).

[26] J. Freeland, J. Lang, G. Srajer, R. Winarski, D. Shu, and D. Mills, Rev. Sci. Instrum. **73**, 1408 (2002).

[27] M. Salluzzo, S. Gariglio, D. Stornaiuolo, V. Sessi, S. Rusponi, C. Piamonteze, G. De Luca, M. Minola, D. Marré, A. Gadaleta *et al.*, Phys. Rev. Lett. **111**, 087204 (2013).

[28] S. Valencia, A. Crassous, L. Bocher, V. Garcia, X. Moya, R. Cherifi, C. Deranlot, K. Bouzehouane, S. Fusil, A. Zobelli *et al.*, Nat. Mater. **10**, 753 (2011).

[29] F. Y. Bruno, J. Garcia-Barriocanal, M. Varela, N. Nemes, P. Thakur, J. Cezar, N. Brookes, A. Rivera-Calzada, M. Garcia-Hernandez, C. Leon *et al.*, Phys. Rev. Lett. **106**, 147205 (2011).

[30] P. Carra, B. Thole, M. Altarelli, and X. Wang, Phys. Rev. Lett. **70**, 694 (1993).

[31] J.-H. Park, E. Vescovo, H.-J. Kim, C. Kwon, R. Ramesh, and T. Venkatesan, Phys. Rev. Lett. **81**, 1953 (1998).

[32] J. Kavich, M. Warusawithana, J. Freeland, P. Ryan, X. Zhai, R. Kodama, and J. Eckstein, Phys. Rev. B **76**, 014410 (2007).

[33] This is well illustrated by another example in Ref. 25 (Figs. 4 and 5). When the magnetic depth profile changes slightly, the simulated x-ray magnetic scattering (dichroic reflectivity here) shows significant changes as a function of energy, while the line shape of the magneto-optical coefficient is kept constant. The imaginary part of the magneto-optical coefficient relates to XMCD, as measured by dichroic TEY here.

[34] T. Y. Chien, L. F. Kourkoutis, J. Chakhalian, B. Gray, M. Kareev, N. P. Guisinger, D. A. Muller, and J. W. Freeland, Nat. Commun. **4**, 2336 (2013).